How to cite: *Angew. Chem. Int. Ed.* **2024**, *63*, e202413977
doi.org/10.1002/anie.202413977

Molecular Shuttles

Cascading Macrocycle and Helix Motions in a Foldarotaxane Molecular Shuttle

Robin Hess[+], Marius Brenet[+], Haingo Rajaonarivelo[+], Maxime Gauthier, Victor Koehler, Philip Waelès, Ivan Huc, Yann Ferrand, and Frédéric Coutrot**

Abstract: The design of a dynamically assembled foldarotaxane was envisioned with the aim of operating as a two cascading trigger-based molecular shuttle. Under acidic conditions, both the macrocycle and helix were localized around their respective best molecular stations because they are far enough from each other not to alter the stability of complexes. The pH-dependent localization of the macrocycle along the encircled axle allowed us to modulate the association between the helical foldamer and its sites of interaction on the axle. Under kinetic control—at low concentration and room temperature—when the foldarotaxane supramolecular architecture is kinetically stable, the pH-responsive translation of the macrocycle along the thread triggered the gliding of the helix away from its initial best station. At higher concentration—when helix assembly/disassembly process is accelerated—the system reached the equilibrium state. A new foldarotaxane isomer then appeared through the change of the relative position of the helix and macrocycle along the thread. In this isomer, the helix segregated the macrocycle away from its best station. The fine control of the kinetic and thermodynamic processes, combined with the control of pH, allowed the reciprocal segregation of the helix or the ring away from their respective best sites of interaction.

Interlocked systems consisting of multiple subcomponents that are maintained thanks to a mechanical bond,[1] make up a class of interwoven molecular architectures that are as aesthetics as they are intriguing. In particular, their physical and chemical properties may highly differ from those of their non-interlocked analogues. In rotaxane architectures—i.e. molecular thread/axle(s) surrounded by macrocycle(s)—the possible mobility of the macrocycle along the thread inspired the conception of numerous multi-stable molecular shuttles and switches.[2] In these systems, motion may take place in response to an external stimulus, according to invertible changes of affinity of the surrounding macrocycle for discrete binding sites—i.e. molecular stations—of the thread. As a source of inspiration for chemists, nature abounds with examples of sophisticated molecular machines that operate through coordinated events and motions.[3] They often work out of equilibrium, involving endergonic physicochemical processes that are fueled by exergonic processes.[4] A high level of sophistication is achieved when movements are orchestrated, that is to say, when a controlled molecular motion induces the motion of another molecule or another part of the same molecule. However, few artificial systems capable of orchestrated motions have been reported.[5] To the best of our knowledge, no molecular shuttle has been shown to operate in response to an external stimulus through the combination of interdependent translational motions of two interlaced elements along a thread. In this article, we report on such an original molecular shuttle based on a pH-sensitive foldarotaxane[6]—i.e. a dynamically-assembled architecture composed of a molecular axle encircled by a macrocycle and entwined with a foldamer helix (Figure 1c). Beyond the sophisticated and rare supramolecular architecture, the novelty stems from the use of the pH-dependent shuttling of the macrocycle along the thread to modulate the association between the foldamer and its sites of interaction, thus triggering kinetically or thermodynamically controlled foldamer motion.

The intended molecular axle of [2]rotaxane **2-HPF$_6$** and foldarotaxane **1⊃2-HPF$_6$** holds bulky aryl extremities—termed stoppers—to preserve the mechanically interlocked [2]rotaxane architecture when the thread is encircled by the

[*] R. Hess,[+] Dr. V. Koehler, Dr. Y. Ferrand
Institut de Chimie et Biologie des Membranes et Nano-objets
CBMN (UMR5248)
Université de Bordeaux, CNRS, IPB
2 rue Robert Escarpit, 33600 Pessac, France
E-mail: yann.ferrand@u-bordeaux.fr
M. Brenet,[+] H. Rajaonarivelo,[+] Dr. M. Gauthier, Dr. P. Waelès, Dr. F. Coutrot
Supramolecular Machines and Architectures Team, IBMM
Université de Montpellier, CNRS, ENSCM, Montpellier, France
E-mail: frederic.coutrot@umontpellier.fr
Homepage: www.glycorotaxane.com
Prof. I. Huc
Department of Pharmacy
Ludwig-Maximilians-Universität
Butenandtstr. 5–13, 81377 München, Germany
[+] These authors contributed equally to this work.

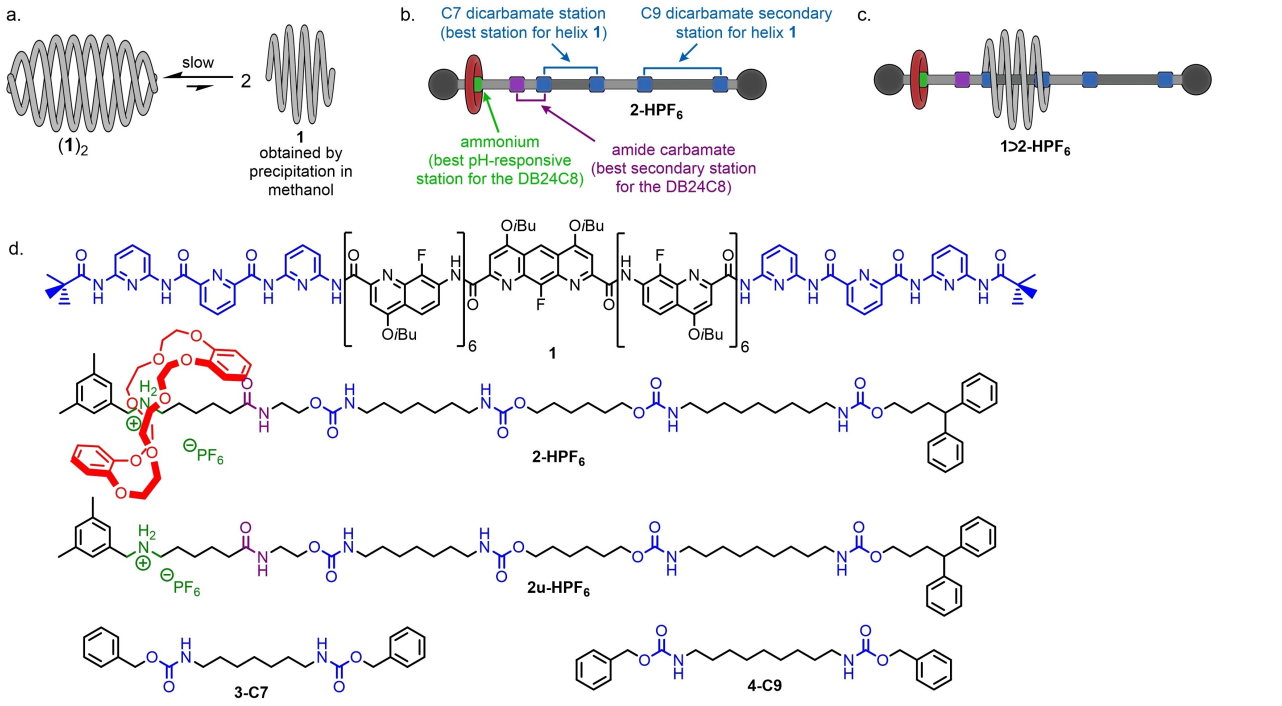

Figure 1. Schematic representations of: a) the equilibrium between double and single helix **1**; b) [2]rotaxane **2-HPF$_6$** and c) foldarotaxane **1⊃2-HPF$_6$**. d) Chemical structures of helix **1**, protonated [2]rotaxane **2-HPF$_6$**, uncomplexed thread **2u-HPF$_6$**, C7 and C9 molecular station-containing models **3-C7 and 4-C9**.

dibenzo-24-crown-8 (DB24 C8) (Figure 1b–d). The encircled axle of **2-HPF$_6$** also contains two favored sites of interactions for the DB24 C8 macrocycle and two sites of interactions for helix **1** (Figure 1b–d). The best molecular station for the DB24 C8 consists of an ammonium[7] moiety (in green), while its best secondary station (in purple and blue) is made of both an amide[8] and a carbamate[9] moieties. The axle also contains three additional carbamate groups. The two pairs of carbamates constitute two molecular stations of different affinity for helix **1**. The insulated seven-methylene-long dicarbamate station (C7) is known for its better affinity towards **1** than the nine-methylene-long dicarbamate station (C9) (Figure 1b, blue).[10] Importantly, it is worth noting that one of the C7 anchoring carbamates may be shared by the helix and the macrocycle in the deprotonated state, the two surrounding subcomponents thus competing for this site at this stage (Figure 1b, purple).

Foldarotaxanes **1⊃2-HPF$_6$** can be formed via the slow winding of single helix **1** around [2]rotaxane **2-HPF$_6$**.[11] The affinity of helix **1** for the axle is controlled by the length of the alkyl spacer (i.e. numbers of methylene units) that separates each carbamate group, the affinity of C7 station being at least one order of magnitude higher than for C9 station. Beyond the preservation of the mechanical bond between the encircled axle and the DB24 C8, the axle stoppers make the supramolecular complex **1⊃2-HPF$_6$** kinetically stable at room temperature, whereas it may disassemble only through a slower unwinding-rewinding process at a higher temperature. The stoppers therefore allow the segregation between the fast gliding of **1** between the C7 and C9 stations and the slow disassembly process between **1** and **2-HPF$_6$**. Based on this knowledge, we first devised that the DB24 C8 shuttling from its best (Figure 2b-I, ammonium, green) to its second-best station (amide-carbamate, purple) would decrease the helix affinity for the C7 station, possibly first inducing its shuttling toward the C9 station via a fast gliding motion[12] to yield a kinetic product. We also envisaged a subsequent slow return of **1** to the C7 station via helix assembly/disassembly process around the rotaxane axle (Figure 2b-II and III).

[2]rotaxane **2-HPF$_6$** was obtained by post-synthetic[13] elongation of an active ester-containing rotaxane building block (Scheme S1–S3).[8,14] Addition of acid or base was carried out to study the shuttling of the DB24 C8 along the encircled thread (Figure 2a). ^{1}H NMR spectra revealed that in the protonated state of the rotaxane axle **2-HPF$_6$**, the DB24 C8 macrocycle resides around the ammonium station, while as expected it shuttles toward the next amide-carbamate main localization upon deprotonation (Figure S1). Foldarotaxane **1⊃2-HPF$_6$** was then obtained through the winding of helix **1** around **2-HPF$_6$** (Figure 2b). The equilibrium, 97 % conversion of **1** into **1⊃2-HPF$_6$**, was reached after stirring **1** (1 mM in CD_2Cl_2) with an excess of [2]rotaxane **2-HPF$_6$** (12.5 mM) at 310 K for 6 days. The formation of **1⊃2-HPF$_6$** was followed by monitoring the helix amide ^{1}H NMR signals region after dilution in dichloromethane at 293 K (Figure S2). The number of helix amide ^{1}H NMR signals of foldarotaxane **1⊃2-HPF$_6$** is double that of **1** (9 N*H*→18 N*H*) due to the unsymmetrical nature of the thread. At equilibrium, the amide resonances of **1**

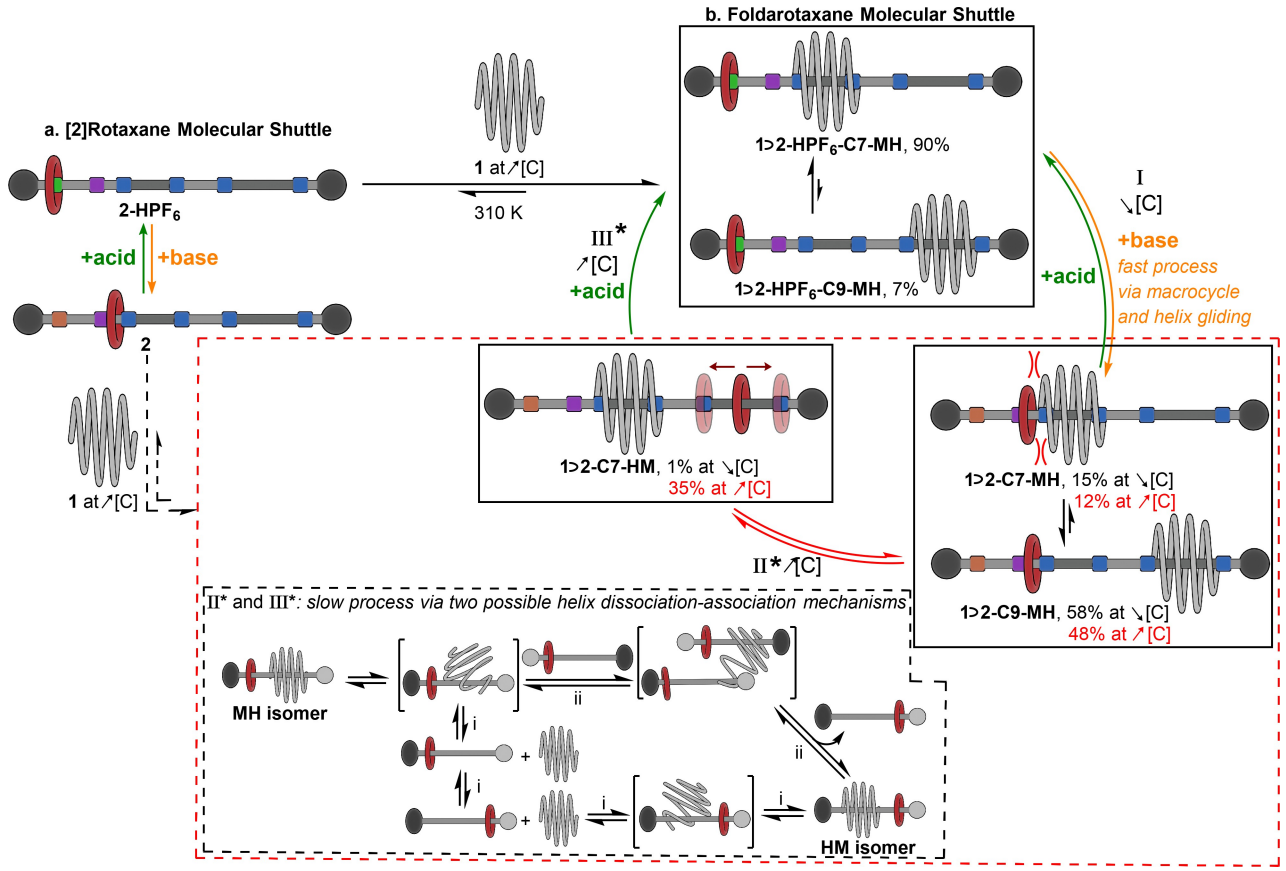

Figure 2. a) Operation of the pH-sensitive [2]rotaxane molecular shuttle **2-HPF$_6$**. b) Operation of the pH- and/or concentration-responsive foldarotaxane molecular machine **1⊃2-HPF$_6$** at 293 K: (I) under kinetic control at a concentration of 0.1 mM, as a pH-responsive foldarotaxane molecular shuttle, through translation of the macrocycle that induces translation of the helix; (II) under thermodynamic control at a higher concentration (1 mM), through disassembly/assembly process of the helix that induces partial relocation of the macrocycle; (III) by adding an acid under thermodynamic control at a concentration of 1 mM, through a disassembly/assembly process of the helix that induces the return to the initial state. The C7 or C9 tag is related to the localization of the helix around the C7 or C9 dicarbamate station, respectively. The MH and HM tags correspond to the relative position of the macrocycle (M) and the helix (H) units with respect to the amine/ammonium moiety. Note that the sum of percentages does not reach 100%, the difference being the percentage of free single helix **1**. ↗[C] stands for 1.0 mM and ↘[C] stands for 0.1 mM.

were replaced by two new sets of signals corresponding to two co-conformers of foldarotaxane **1⊃2-HPF$_6$**, for which the helix was located either around the C7 or the C9 stations (Figure 3a–b). The assignment of the NMR signals to each co-conformer was based on a comparison with the spectra of model foldaxanes[15] **1⊃3-C7** and **1⊃4-C9** (Figure 1d and Figure S3–S4). These compounds contain either a C7 or a C9 station for helix **1** and show distinct ^{1}H NMR patterns (Figure S2).

As expected, for **1⊃2-HPF$_6$**, the helix prefers to stay on the C7 station (90% of co-conformer **1⊃2-HPF$_6$-C7-MH**) than on the C9 station (7% of co-conformer **1⊃2-HPF$_6$-C9-MH**). The same preference (ratio of 93/7 for C7/C9 stations) was observed for the winding of **1** around the uncomplexed thread **2u-HPF$_6$** (Figure S2). This hints at an absence of effect of DB24 C8 on the position of **1** when the macrocycle is located around the ammonium, that is, far enough from the nearest station of the helix.

We then envisioned the cascading translation of the helix along the thread induced by the pH-dependent macrocycle translation. A decrease in the association between the helix and the C7 station was expected when the macrocycle competed with that station.[6a] This should therefore trigger the gliding of the helix around the C9 station. Deprotonation of the ammonium by a strong base (phosphazene base 2-*tert*-butylimino-2-diethylamino-1,3-dimethylperhydro-1,3,2-diazaphosphorine supported-resin) was first achieved at low concentration (0.1 mM) and 293 K, actuating the macrocycle shuttling towards the amide-carbamate station (in purple and blue, respectively; in Figure 2b-I). Accordingly, the positioning of the helix at the C9 station became more populated in the deprotonated state **1⊃2**. After 250 min, both kinetic co-conformers **1⊃2-C7-MH** and **1⊃2-C9-MH** (15:58) were observed, along with the partial dissociation of **1** (26%). In short, releasing the macrocycle from its ammonium binding site results in an overall change of position of the helix. Meanwhile, the release of **1** upon deprotonation could be attributed to the displacement of the equilibrium towards the disassembled elements, due to the dilution of the reaction mixture (from 1 mM for the

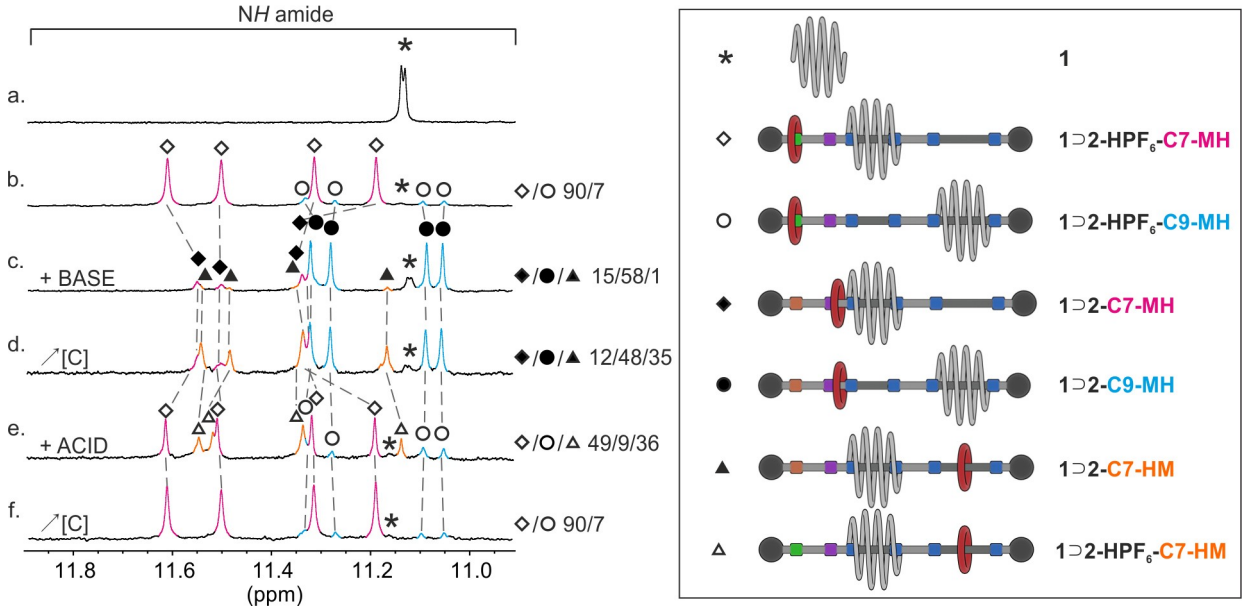

Figure 3. Sections of ^{1}H NMR spectra (700 MHz, CD_2Cl_2, 0.1 mM, 298 K) showing the characteristic amide resonances of: a) free single helix **1** (black star) obtained by precipitation in methanol, b) foldarotaxane **1⊃2-HPF$_6$** obtained by stirring **1** (1 mM) with **2-HPF$_6$** (12,5 equiv.) at 310 K for 6 days. **1⊃2-HPF$_6$-C7-MH** and **1⊃2-HPF$_6$-C9-MH** are denoted with empty diamonds and empty circles, respectively. MH and HM denote the relative positions of the macrocycle vs the helix (left or right). ^{1}H NMR spectra of **1⊃2** following deprotonation of the ammonium moiety using 2-*tert*-butylimino-2-diethylamino-1,3-dimethylperhydro-1,3,2-diazaphosphorine supported-resin (625 equiv.) at 293 K after: c) 250 min at 0.1 mM, and d) 6 days at 1 mM. New foldarotaxane isomers are denoted as follows: **1⊃2-C7-MH** (c, pink resonances, black filled diamonds), **1⊃2-C9-MH** (c, blue resonances, black filled circles), and **1⊃2-C7-HM** (d, orange resonances, black filled triangles). ^{1}H NMR spectra of the reprotonation of thermodynamic mixture obtained in (d) using NH_4PF_6 (188 mM) after: e) 5 h at 0.1 mM (new foldarotaxane isomer **1⊃2-HPF$_6$-C7-HM** is denoted by empty triangles) and f) 8 days at 1 mM. ↗[C] stands for an increase in concentration to 1.0 mM.

foldarotaxane formation to 0.1 mM for the deprotonation). Another reason is the lesser affinity of **1** for the C9 station or for the C7 one when it is occupied by the DB24 C8. Moreover, since unwinding-based disassembly of the helix out of the rod is slow at low concentration and 293 K, one may also suggest that the DB24 C8 squeezes the helix to supplement energy for helix unwinding out from the C7 station.

^{1}H NMR evidence of these cascading interdependent motions are shown in Figure 3b–c. Since all the foldarotaxane co-conformers are in slow exchange on the ^{1}H NMR time scale, variation of their proportion over time could be followed by direct integration of the proton signals (Figure S5–S7). Upon deprotonation, the intensity of low field amide set of resonances of **1** located on the C7 station (**1⊃2-HPF$_6$-C7-MH**) decreased progressively over time. Meanwhile, a new species emerged at a higher field corresponding to the helix on the C9 station (**1⊃2-C9-MH**). A careful examination of the chemical shift variations allowed to discriminate **1⊃2-C7-MH** from **1⊃2-HPF$_6$-C7-MH**. This observation corroborated the change of environment around the C7 station, due to the proximity between DB24 C8 and **1** in **1⊃2-C7-MH**. On the contrary, **1⊃2-HPF$_6$-C9-MH** and **1⊃2-C9-MH** have similar chemical shift values (Figure 3b–c), in agreement with the more distant location of DB24 C8 from **1** in both species. The molecular structure of each co-conformer was validated using molecular mechanics (Figure S8).

At higher concentration (1 mM), the rate of helix translocation between isomers MH and HM was increased, allowing the system to reach thermodynamic equilibrium after about 6 days (Figure S9–S10). Unlike in the steady-state reached at low concentration, helix disassembly and reassembly allowed for DB24 C8 and helix **1** to swap faster their relative positions on the thread through intermolecular process.[16] Thus, a new foldarotaxane isomer **1⊃2-C7-HM** was formed in a significant proportion. In **1⊃2-C7-HM**, helix **1** resided on the C7 station, while DB24 C8 had translocated on the carbamates of the C9 station. The three coexisting co-conformers, **1⊃2-C7-MH**, **1⊃2-C9-MH**, and **1⊃2-C7-HM** were then found in a 12:48:35 proportion, while 5% of unbound **1** was still present (Figure S9–S10). The ratio between **1⊃2-C7-HM** and **1⊃2-C7-MH** reflects that, when the C7 station is occupied by the helix, DB24 C8 interacts with the two carbamates of the C9 station better than with the amide. When the helix lies on the C7 station, it thus biased the DB24 C8 populations between its main sites of interactions. Conversely, the prevalence of **1⊃2-C9-MH** indicates that the apparent affinity of the helix for the C7 station is still reduced by the competition with the macrocycle for that same station, but to a lesser extent than in the stationary state obtained immediately after deprotonation.

Return to the initial state through reprotonation was then implemented (Figure S11–S16). Since protonation of the helix pyridyl pinchers would cause the unwanted disassembly of the foldarotaxane, selective protonation of

the thread amine moiety was carried out carefully in dichloromethane using the weak Brønsted acid ammonium hexafluorophosphate. Protonation of the foldarotaxane co-conformers of **1⊃2** obtained either under the kinetic or thermodynamic control was monitored by ^{1}H NMR (Figure 3e-f). Unsurprisingly, protonation of the steady-state mixture obtained after deprotonation at 0.1 mM, **1⊃2-C7-MH**:**1⊃2-C9-MH** (15:58), reversed back over time to the initial protonated state, that is, **1⊃2-HPF$_6$-C7-MH**:**1⊃2-HPF$_6$-C9-MH** (93:7) (Figure 2b-I and S11–S12). We then focused with more curiosity on the protonation at low concentration (0.1 mM) of the mixture of isomers obtained after deprotonation at the higher concentration (1 mM) **1⊃2-C7-MH**:**1⊃2-C9-MH**:**1⊃2-C7-HM** (12:48:35) (Figure 2b-III and S13–S14). After 290 min at low concentration, when disassembly/assembly process of the helix around the axle is negligible, protonation led to the mixture of foldarotaxanes **1⊃2-HPF$_6$-C7-MH**:**1⊃2-HPF$_6$-C9-MH** 49:9 (Figure 3e). Noteworthy, we also observed the presence of the metastable protonated foldarotaxane intermediate **1⊃2-HPF$_6$-C7-HM** (36 %), for which the helix acted as a kinetic supramolecular barrier[17] that compartmentalized the foldarotaxane subcomponents and prevented DB24 C8 from shuttling back to its favored ammonium station. At the higher concentration (1 mM), this barrier effect of the helix was not observed anymore as **1** could disassemble and reassemble faster around the axle,[16] thus allowing the DB24 C8 to reach its initial ammonium station. In these conditions, the co-conformers **1⊃2-HPF$_6$-C7-MH**:**1⊃2-HPF$_6$-C9-MH** were produced in the ratio 93:7 after 8 days (Figure 3f, S15–S16).

In conclusion, interdependent cascading motions of two discrete surrounding units—a macrocycle and a helix—along a thread in a foldarotaxane architecture were successfully performed thanks to pH stimuli at variable concentrations. At room temperature, translation of a macrocycle inducing translation of a helix at low concentration, combined with the faster disassembly/assembly process[16] of the helix at a higher concentration, resulted in a very appealing and original compartmentalized supramolecular shuttle, in which both helix and macrocycle could be trapped around regions of the axle for which they have less affinity. On the one hand, controlling the main localization of the macrocycle along the thread allowed for modulating the competition of both helix and macrocycle for the same site, thus impacting the position of the helix. The pH-sensitive shuttling of the macrocycle along the thread at room temperature significantly biased—even reversed—the helix population on its two sites of interaction (C7 vs C9), until a stationary state was reached. On the other hand, the helix showed reciprocally an effect on the macrocycle localization. Indeed, equilibrium between isomers was reached at higher concentration, thanks to the relative positions swapping of the helix and macrocycle. Notably, this location exchange afforded isomers (**1⊃2-C7-HM** followed by **1⊃2-HPF$_6$-C7-HM** after mild reprotonation) for which the helix sequestrated the macrocycle around a part of the thread whose affinity is less in the absence of the helix. Relaxation over time at higher concentration allowed for returning to the initial state. Such a supramolecular architecture that operates through successive interdependent motions paves the way to the design of original supramolecular ratcheting[18] systems in which the helix subcomponent may act as a supramolecular kinetic barrier to sequestrate the macrocycle away from its best site of interaction.

Acknowledgements

We thank the "Agence Nationale de la Recherche" for funding the project ANR-17-CE07-0014-01 and the France-Germany International Research Project "Foldamers Structures and Functions" (IRP FoldSFun).

Conflict of Interest

The authors declare no conflict of interest.

Data Availability Statement

The data that support the findings of this study are available in the supplementary material of this article.

Keywords: foldamers · foldarotaxanes · molecular shuttles · rotaxanes · self-assembly

[1] C. J. Bruns, J. F. Stoddart, *The nature of the mechanical bond: From Molecules to Machines*, Wiley, Hoboken, **2016**.

[2] a) S. Erbas-Cakmak, D. A. Leigh, C. T. McTernan, A. L. Nussbaumer, *Chem. Rev.* **2015**, *115*, 10081–10206; b) H.-Y. Zhou, Y. Han, C.-F. Chen, *Mater. Chem. Front.* **2020**, *4*, 12–28; c) M. Baroncini, S. Silvi, A. Credi, *Chem. Rev.* **2020**, *120*, 200–268; d) S. Kassem, T. van Leeuwen, A. S. Lubbe, M. R. Wilson, B. L. Feringa, D. A. Leigh, *Chem. Soc. Rev.* **2017**, *46*, 2592–2621; e) S. Zhang, Y. An, X.-M. Chen, Q. Li, *Smart Molecules.* **2023**, *1*, e20230015; f) J.-P. Sauvage, P. Gaspard, *From non-covalent assemblies to molecular machines*, Wiley-VCH, **2011**.

[3] F. Lancia, A. Ryabchun, N. Katsonis, *Nat. Chem. Rev.* **2019**, *3*, 536–551.

[4] a) S. Corra, M. Curcio, A. Credi, *J. Am Chem. Soc. Au* **2023**, *5*, 1301–1313; b) E. Olivieri, J. M. Gallagher, A. Betts, T. W. Mrad, D. A. Leigh, *Nat. Synth.* **2024**, *3*, 707–714; c) M. Stasi, H. Soria-Carrera, J. Boekhoven, *Nat. Synth.* **2024**, *3*, 673–674; d) S. Al Shehimy, H.-D. Le, S. Di Noja, S. Amano, L. Monari, G. Ragazzon, preprint at doi: 10.26434/chemrxiv-2024-4krgj-(2024).

[5] a) T. Muraoka, K. Kinbara, T. Aida, *Nature* **2006**, *440*, 512–515; b) E. Okuno, S. Hiraoka, M. Shionoya, *Dalton Trans.* **2010**, *39*, 4107–4116; c) J. .-J. Yu, L. .-Y. Zhao, Z. .-T. Shi, Q. Zhang, G. London, W. .-J. Liang, C. Gao, M. M. Li, X. .-M. Cao, H. Tian, B. L. Feringa, D. .-H. Qu, *J. Org. Chem.* **2019**, *84*, 5790–5802; d) Y. Wang, Y. Tian, Y. .-Z. Chen, L. .-Y. Niu, L. .-Z. Wu, C. .-H. Tung, Q. .-Z. Yang, R. Boulatov, *Chem. Commun.* **2018**, *54*, 7991–7994; e) F. Coutrot, E. Busseron, *Chem. Eur. J.* **2009**, *15*, 5186–5190; f) D. A. Leigh, J. K. Y. Wong, F. Dehez, F. Zerbetto, *Nature* **2003**, *424*, 174–179; g) E. Elramadi, S. Kundu, D. Mondal, T. Paululat, M. Schmittel, *Angew. Chem. Int. Ed.* **2024**, e202404444.

[6] a) M. Gauthier, V. Koehler, C. Clavel, B. Kauffmann, I. Huc, Y. Ferrand, F. Coutrot, *Angew. Chem. Int. Ed.* **2021**, *60*, 8380–8384; *Angew. Chem.* **2021**,*133*, 8461–8465; b) V. Koehler, M. Gauthier, C. Yao, K. Fournel-Marotte, P. Waelès, B. Kauffmann, I. Huc, F. Coutrot, Y. Ferrand, *Chem. Commun.* **2022**, *58*, 8618–8621.
[7] A. G. Kolchinski, D. H. Busch, N. W. Alcock, *J. Chem. Soc. Chem. Commun.* **1995**, 1289–1291.
[8] B. Riss-Yaw, J. Morin, C. Clavel, F. Coutrot, *Molecules* **2017**, *22*, 2017.
[9] P. Waelès, M. Gauthier, F. Coutrot, *Eur. J. Org. Chem.* **2022**, e202101385.
[10] X. Wang, Q. Gan, B. Wicher, Y. Ferrand, I. Huc, *Angew. Chem. Int. Ed.* **2019**, *58*, 4205–4209; *Angew. Chem.* **2019**, *131*, 4249–4253.
[11] For other examples relative to the formation of foldarotaxane and foldaxane utilizing helix **1**, see ref 6a and 12.
[12] Noteworthy, foldaxane molecular shuttle based on the translation of a foldamer helix along a molecular rod has only been reported once, see: Q. Gan, Y. Ferrand, C. Bao, B. Kauffmann, A. Grélard, H. Jiang, I. Huc, *Science* **2011**, *331*, 1172–1175.
[13] P. Waelès, M. Gauthier, F. Coutrot, *Angew. Chem. Int. Ed.* **2021**, *60*, 16778–16799; *Angew. Chem.* **2021**, *133*, 16916–16937.
[14] a) T. Legigan, B. Riss-Yaw, C. Clavel, F. Coutrot, *Chem. Eur. J.* **2016**, *22*, 8835–8847; b) B. Riss-Yaw, T. X. Métro, F. Lamaty, F. Coutrot, *RSC Adv.* **2019**, *9*, 21587–21590.
[15] V. Koehler, A. Roy, I. Huc, Y. Ferrand, *Acc. Chem. Res.* **2022**, *55*, 1074–1085.
[16] Two intermolecular mechanisms are possible to interconvert isomers MH and HM, either via disassembly-then-reassembly of the complex helix-rotaxane, or via intermolecular translocation of the helix from foldarotaxane to rotaxane species, as illustrated in Figure 2.
[17] E. R. Kay, D. A. Leigh, F. Zerbetto, *Angew. Chem. Int. Ed.* **2007**, *46*, 72–191; *Angew. Chem.* **2007**, *119*, 72–196.
[18] S. Borsley, J. M. Gallagher, D. A. Leigh, B. M. W. Roberts, *Nat. Chem. Rev.* **2024**, *8*, 8–29.

Manuscript received: July 24, 2024
Accepted manuscript online: September 9, 2024
Version of record online: October 30, 2024